COBEM UBERLÂNDIA 2019

ABCM Associação Brasileira de Engenharia e Ciências Mecânicas

25th ABCM International Congress of Mechanical Engineering
October 20-25, 2019, Uberlândia, MG, Brazil

COB-2019:0111 PRODUCTION WELL LAYOUTS GUIDED BY MULTIPLE ROCK CLUSTERING AND PERMEABILITY AVERAGING RULES

Gustavo P. Oliveira
Lucas C. Silva
Marcos R. B. dos Santos
Waldir L. Roque
Petroleum Engineering Modelling Laboratory, Federal University of Paraíba, João Pessoa, Brazil
gustavo.oliveira@ci.ufpb.br, lucascavalcanti@ufpb.ct.br, marcosramon.98@gmail.com, roque@ci.ufpb.br

Abstract. *This paper is intended to study the 3D modeling of hydraulic flow units and associated well placement layouts applicable to heterogeneous oilfields. We present a clusterwise approach that seeks to identify volumes that confine "sweet spots" taking into account two versions for the flow zone indicator, namely FZI and FZI*, which are quantities statistically distributed throughout the porous medium and computed through linear regression. Rock clusters are determined by using distinct permeability averaging rules in order to verify the responses of the clustering in locating high fluidity zones. Additionally, production wells are placed strategically at points determined by each approach. Layouts are then contrasted after performing long term flow simulations in a fully implicit black-oil solver provided by the MRST (Matlab Reservoir Simulation Toolbox) toolbox. We have concluded that the permeability averaging rules have a considerable impact over the produced oil volume not only for layouts obtained with the same flow indicator, but also for layouts compared vis-à-vis between the two flow indicators.*

Keywords: *reservoir modelling, hydraulic flow units, flow zone indicator, clustering.*

1. INTRODUCTION

Exploration and production activities in the oil and gas industry are the front-line in the matter of leveraging hydrocarbon recovery processes both from onshore and offshore reserves. During the stages of field development, well drilling and completion correspond to a large budget of capital and operational expenditures in a company. Actions that aim to reduce costs with implementing intelligent field designs and smart production strategies are, in turn, of uttermost importance.

Over the years, research efforts have been dedicated to laying out workflows, processes and guidelines that may be universally applicable to a wide range of geologic formations for the purpose of characterizing reservoirs. In this context, it arises the necessity of identifying hydrocarbon-bearing regions whose production rates uplift the return on investment. Under the engineering's viewpoint, volumetric regions capable to correspond to such expectations are termed *hydraulic flow units* (HFUs). Generally, HFUs are reservoir rock portions whose petrophysical and flow properties are similar (Tiab and Donaldson, 2011). In turn, they represent target zones for ultimate harnessing.

The accurate determination of HFUs, as well as the search for suitable locations wherein producer wells should be placed is a subject discussed in several papers that cope with this problem usually backed by optimization algorithms and objective functions as reported by (Bangerth *et al.*, 2006), (Nasrabadi *et al.*, 2012), (Rahmanifard and Plaksina, 2018) and many others. Currently, this problem has been captivating researchers acquainted with artificial intelligence, data-driven methods and hybrid formulations.

Recently, Oliveira *et al.* (2016) and Roque *et al.* (2017) developed a technique to delineate HFUs based on a kind of clustering followed by well placement selection from graph theory and centrality measures. In these papers, the flow zone indicator (FZI) was the parameter used as primary variable to establish a discrete transform that labels several clusters of rocks distinctly. On the other hand, novel approaches have been arising and shedding light on proper ways to identify HFUs in reservoirs, as discussed in (Mirzaei-Paiaman *et al.*, 2018) and (Mirzaei-Paiaman *et al.*, 2019).

A modified version of FZI, termed FZI* (FZI-Star), was introduced by Mirzaei-Paiaman *et al.* (2015) as an alternative to known indices. As with FZI, FZI* can be understood as a physically consistent parameter that embeds petrophysical properties of the porous medium aimed to grade a flow transport "potential". In this paper, we analyze how different is the rock clustering output resulting from FZI and FZI* transforms when combined with distinct fundamental averaging rules to establish an equivalent permeability derived from the principal components of the permeability tensor. Rock clusters are determined by using distinct permeability averaging rules in order to verify the responses of the clustering in locating high fluidity zones. Additionally, production wells are placed strategically at points determined by each approach. Layouts are then contrasted after performing long term flow simulations in a fully implicit black-oil solver provided by MRST toolbox, by which the cumulative oil production is evaluated for each case.

2. METHODOLOGY

2.1 Hydraulic flow units

The generalized Kozeny-Carman's (K-C) equation provides a relationship between the permeability k and the effective porosity ϕ_e of a porous medium from

$$k = \frac{1}{F_s\,\tau^2\,S_{gv}^2}\frac{\phi_e^3}{(1-\phi_e)^2}, \tag{1}$$

where F_s is the grain shape factor, τ the pore tortuosity and S_{gv} the specific surface area per unit grain volume (Carman, 1937). However, to bypass difficulties due to changes of the Kozeny's constant $F_s\tau^2$ among distinct regions of a reservoir, Amaefule *et al.* (1993) presented an alternative way to express the K-C model as

$$\sqrt{\frac{k}{\phi_e}} = \frac{1}{\sqrt{F_s}\tau S_{gv}}\phi_z, \tag{2}$$

where $\phi_z = \frac{\phi_e}{1-\phi_e}$ is called the pore-to-matrix ratio (or normalized porosity). From Eq. (2), two parameters were devised, namely the reservoir quality index (RQI) and the flow zone indicator (FZI), both defined as

$$RQI(\mu m) = 0.0314\sqrt{\frac{k}{\phi_e}} \quad ; \quad FZI = \frac{1}{\sqrt{F_s}\tau S_{gv}}, \tag{3}$$

where 0.0314 is a unit conversion factor used when k is given in millidarcies. By rewriting Eq. (2) with these terms, it now reads as

$$RQI = FZI \times \phi_z, \tag{4}$$

which becomes

$$\log(RQI) = \log(\phi_z) + \log(FZI) \tag{5}$$

after taking the logarithm on both sides. Such expression indicates that in a log-log scatter plot of RQI versus ϕ_z, all the samples with similar FZI values will lie on a best-fit line of unit slope, thus meaning that they correspond to rock samples whose pore throat attributes are similar. A reservoir volume whose geological and petrophysical properties are the same is recognized as a *hydraulic flow unit* (HFU). In particular, for Hearn *et al.* (1984), a HFU is both a laterally and vertically continuous reservoir zone whose permeability, porosity and bedding characteristics are similar. Furthermore, according to Tiab and Donaldson (2011), the HFUs have the following properties: (i) they are a specific volume of reservoir, composed of one or more reservoir quality lithologies; (ii) they are correlative and mappable at the interval scale; (iii) their zonation is recognizable on wire-line log; (iv) they may communicate each other.

2.2 Dynamic flow zone indicator

In Mirzaei-Paiaman *et al.* (2015) and, later on, in Mirzaei-Paiaman *et al.* (2018), the meaning of the FZI was re-designed to be interpreted as a dynamic flow zone indicator termed FZI^*. This is due to a restatement of the reservoir quality index which allows us to replace

$$FZI^* = FZI \times \phi_z = 0.0314\sqrt{\frac{k}{\phi_e}}. \tag{6}$$

The introduction of FZI^* into reservoir characterization workflows is intended to make distinction between static and dynamic HFUs, although it delivers a similar interpretation for the flow potential of a rock unit. The same idea as that developed for FZI holds, except that now a dynamic HFU is recognized when satisfying the linear regression equation

$$\log(0.0314\sqrt{k}) = \log(\sqrt{\phi_e}) + \log(FZI^*) \tag{7}$$

under equivalent criteria of Eq. (5).

2.3 Discrete rock typing

By following the theoretical models of FZI, a 3D discrete rock type technique (from now on, DRT) was proposed by Guo *et al.* (2005) to facilitate the rock type transfer to simulation models. The formula is given by

$$DRT^{(*)} = \text{round}(2\ln(FZI^{(*)}) + 10.6), \tag{8}$$

which performs a conversion from the continuous approach based on FZI (or FZI*) to synthetic log data so as to allow a complete classification of the reservoir under study. Each DRT (or DRT^*) is an integer number that labels distinct HFUs and may have a wide enumeration range depending on the geological formation of the reservoir. In our analyses, zero-porosity cells that cause indeterminate DRT (or DRT^*) values in the synthetic model are expunged. Hence, we may compare the outcomes generated from both approaches properly.

2.4 Field layout modelling

To give a simplified view of an oilfield, we introduce here an abstract field layout model $\mathcal{L}$ made up by producer wells only. The oilfield will be treated as a set $\Omega \subset \mathbb{R}^3$ having three main entities: producer wells, perforation zones and HFUs. Respectively, let us consider $\mathcal{W} = \{W_1, W_2, \dots W_p\}$ the set of producer wells, $\mathcal{P} = \{P_1, P_2, \dots P_q\}$ the set of perforation zones and $\mathcal{H} = \{H_1, H_2, \dots H_r\}$ the set of HFUs. Furthermore, we allow that a given perforation zone may be sectioned into n parts, i.e. $P_i = P_{i1} \cup P_{i2} \dots \cup P_{in}$, for $1 \leq i \leq q$. In brief, the field layout model in Ω is described as

$$\mathcal{L} = \mathcal{W} \times \mathcal{P} \times \mathcal{H}. \tag{9}$$

Figure 1 depicts a scheme having a unique well in the layout model with only one perforation zone as well, which can be replicated throughout Ω. This configuration is extendable in the same manner to include injector wells, for instance.

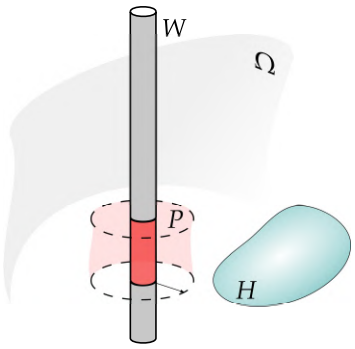

Figure 1. Field layout model $\mathcal{L}$ for an oilfield Ω: W represents a unique well; P represents a region around the borehole which is feasible for perforation operations and H is a volume characterizing a hydraulic flow unit.

2.5 Rock clustering

To map the spatial distribution of the HFUs over the reservoir in order to know their shape, we apply a connectivity criterion by which the interconnected porous medium space may be represented in a discrete form. Here, the reservoir is treated as a set of cells connected by faces. In a 3D reservoir, each discrete cell has its location given by logical Cartesian coordinates – although more realistic models assume the structure of corner-point grids. In this paper, we will be limited only to vertical wellbores, as well as to lateral and vertical connections, mainly towards depth axis κ. The scheme, however, can be adapted for directional wells. We define a $DRT^{(*)}$-based cluster as a structure of connected cells as

$$C_{D,q} \quad := \{w \in \Omega;\, DRT^{(*)}(w) = D \,\wedge\, w \in N_7(w_s)\},\;\; q = 1, 2, \dots, Q, \tag{10}$$

where w is an arbitrary cell of the reservoir domain Ω, N_7 a structuring element formed by a seed cell w_s plus its six face-neighbour cells which provides the dynamic connectivity, q the cluster index and Q the total amount of distinct clusters generated *per* $DRT^{(*)}$ value computed from Eq. (8). Note that each cluster may have a variable number n_q of interconnected cells. Hence, $C_{D,q}$ is a disjoint set that represents a rock volume characterized by similar petrophysical properties.

2.6 Permeability averaging rules

Estimating an equivalent permeability that can be fairly used in discrete schemes to represent heterogeneous and anisotropic porous media is a subtle issue in numerical methods applied to petroleum reservoirs. Although the permeability is a symmetric tensor, its numerical treatment is usually approximated. As pointed out by Renard and de Marsily

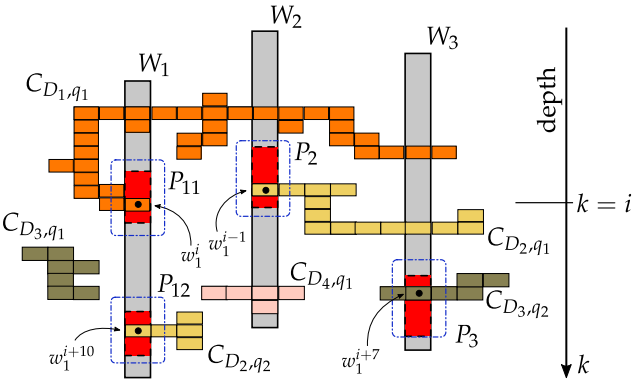

Figure 2. Concept model of rock clustering in a reservoir model: cell connectivity, well-crossing bodies and arbitrary shapes.

(1997), it is impossible to achieve a complete equivalence for the permeability of a heterogeneous medium and a fictitious homogeneous one, so that a proxy constant tensor should play the role of local value for the permeability. Barriers, faults and the overall reservoir architecture exerts severe influence to the permeability ratio. As discussed in Baker *et al.* (2015), different averaging rules should be used according to the layering features and pore disorder found at a heterogeneous reservoir. It is unlikely to have a single rule valid at all scales. In their words, proper choices will depend on the application. That is why several approaches were developed to compute a representative permeability useful in cell-centered schemes and upscaling procedures that carry the permeability behavior to larger scales. In this paper, we have resorted to five fundamental averages that take into account only the principal directions of the permeability tensor $\boldsymbol{K}$. This way, the *arithmetic*, *geometric*, *normalized* (based on the Euclidean vector norm), *harmonic*, and *quadratic* are defined, respectively, by

$$k_a = \frac{1}{3}\sum_{i=1}^{3} K_{ii},\; k_g = \left(\prod_{i=1}^{3} K_{ii}\right)^{1/3},\; k_n = \left(\sum_{i=1}^{3} K_{ii}^2\right)^{1/2},\; k_q = \left(\frac{1}{3}\sum_{i=1}^{3} K_{ii}^2\right)^{1/2} \text{ and } k_h = \frac{3}{\sum_{i=1}^{3} K_{ii}^{-1}}, \tag{11}$$

for which K_{ii} is the i-th principal component of $\boldsymbol{K}$. In fact, such averages are particular cases of the generalized mean. For brevity and data presentation, the subscript α will be used whenever we make reference to a particular equation.

3. RESULTS

3.1 Discrete rock distribution

Below, we present a few results concerning the discretization of the UNISIM-I-D model (Namorado oilfield, Campos Basin, Rio de Janeiro) into rock clustering/permeability averaging pairs. We have added in Fig. 3 the histograms of the quantities DRT and DRT^* for each of the five permeability averages k_α fitted by their associated log-normal distributions $\mathcal{N}_\alpha$. The histograms represent all the nonzero values of discrete rock types found for the model and give a full portrait of the reservoir zoning according to the flow indicator relationships (FZI, at left; FZI^*, at right). We observe some

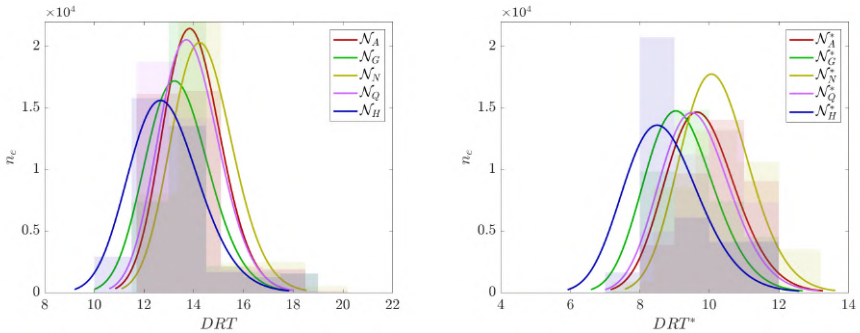

Figure 3. Distribution of rock types over the model computed with all the averaging rules for the flow indicators (FZI, at left; FZI^*, at right).

characteristics in the histograms concerning the number of distinct rock types found over the field and their frequency.

Firstly, it is seen that the range of DRT values covered for all the averaging rules is 10 - 20 (11 types), slightly larger than that for DRT^*, which is 6 - 13 (8 types). Secondly, one verifies that the DRT distribution is more frequent in a few intermediary rock types than the DRT^* distribution. Seemingly, DRT^* presents a better balance of the rock type spreading over the field for all the averaging rules, even with a protrusion of $\mathcal{N}_h^*$. Consequently, a lesser concentration of values is obtained.

We have included a few sieve plots of 3D distributions of the rock types over the whole model in Fig. 4 only for illustration, since it is hard to distinguish the rock types in each case. Similar plots are produced for all the other distributions.

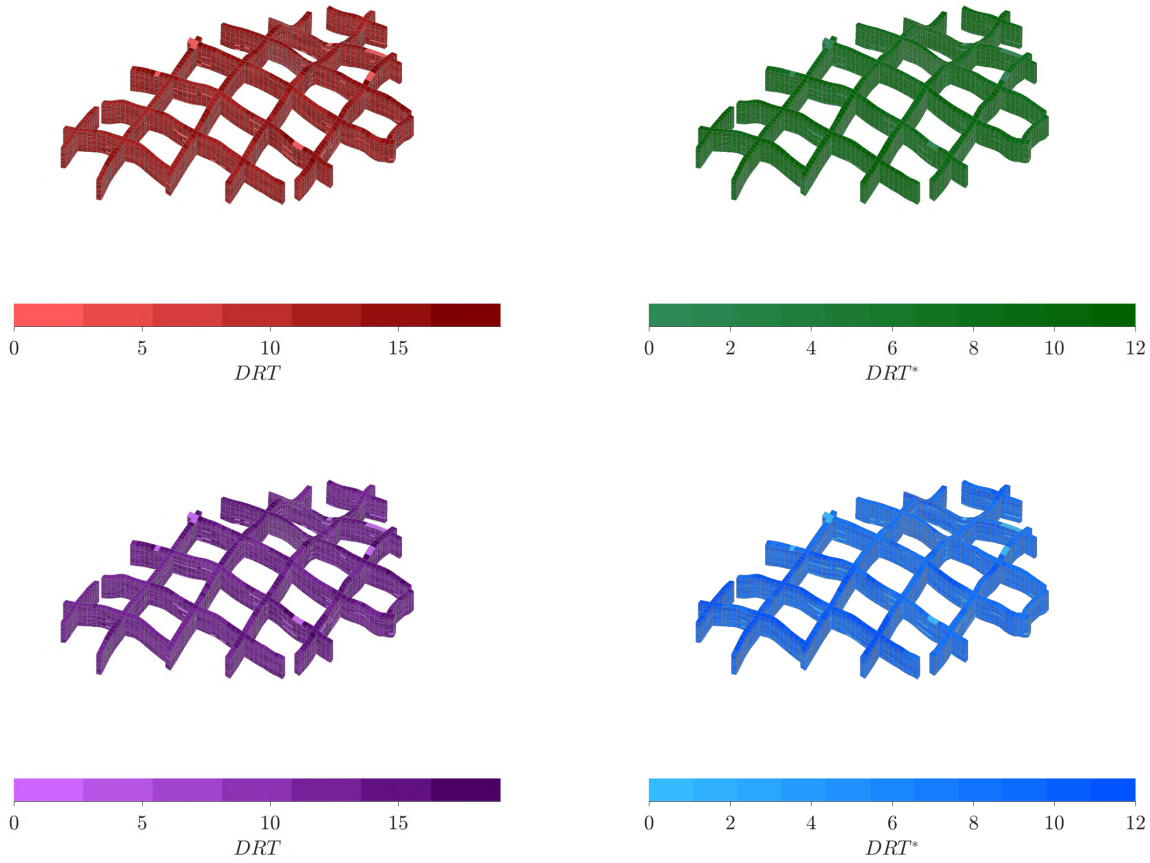

Figure 4. Sieve plot of the 3D distribution of $\mathcal{N}_a$ (top left), $\mathcal{N}_g^*$ (top right), $\mathcal{N}_q$ (bottom left), and $\mathcal{N}_h^*$ (bottom right) over the UNISIM-I-D model.

3.2 High-performance cluster dendograms

Dendograms provide a hierarchical view of clustering. Simplified dendograms are included in this study with an illustrative purpose. Figure 5 shows two dendograms for the DRT and DRT^* distributions, respectively. Each permeability rule (k_α) occupies the first row. Rock type values follow in the second row. In last, we report, for the specified rock type, the total number of high-performance clusters ($\#C$) whose minimum number of cells is 5. High-performance clusters fulfill analytic requirements that are discussed in Roque *et al.* (2017). Highlight colors are assigned only for those rock types – per averaging rule family – that are predominant in terms of clusters. For instance, $DRT = 12$ is more abundant when $\alpha = q$ because it has 16 clusters, against 6, 5, and 3, produced by $DRT = 14$, $DRT = 15$, and $DRT = 16$, respectively. The rock clustering procedure shows that, due to a more dispersed behavior, the DRT approach estimates a number considerably higher of clusters than the DRT^* approach, which is more compact. That is to say, for all averaging rules, the rock typing is more parsimonious for the DRT^* approach. For example, k_n produces 6 rock types through DRT, but half of that through DRT^*. Likewise, k_a produces 5 rock types through DRT, but only 3 through DRT^*. In terms of field coverage, this means that the DRT approach delivers a broader area for well placement strategy and planning. However, the quality of the layouts produced by the DRT^* clustering may reveal itself better in respect to production. This will be examined later. Differences of rock typing produced by different approaches is a promising subject for characterization

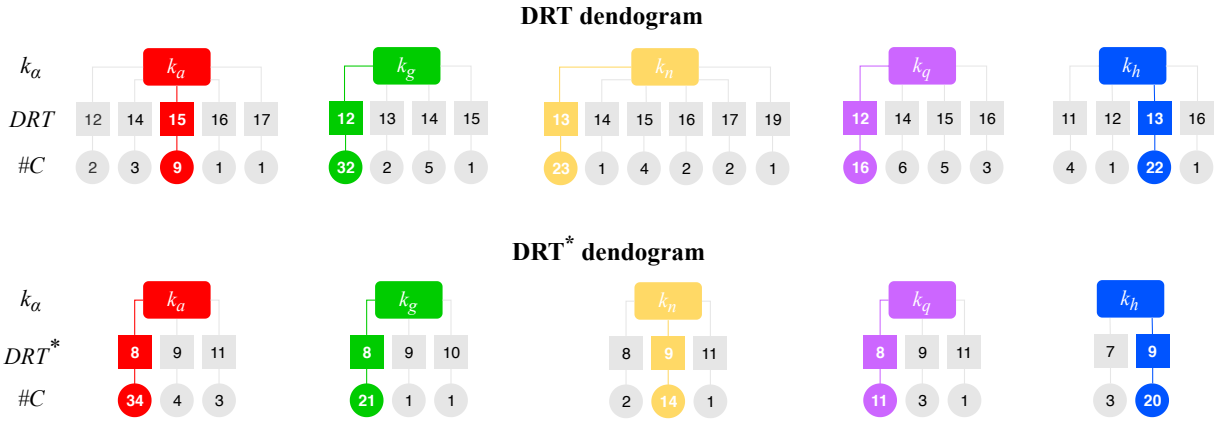

Figure 5. Dendograms of high-performance clusters for the DRT and DRT^* distributions. In the first row, k_α is the averaging rule. The rock type approach follows in the second row. Next, the total number of high-performance clusters $\#C$ appears in the third row. Highlights emphasize the predominant rock types for each rule.

of heterogeneous reservoirs, since several dynamic and static properties should be considered. Recently, by following the FZI and FZI^* approaches, Soleymanzadeh *et al.* (2019) concluded that effects of the overburden pressure, for instance, induce trends in measurements and modify the nature of the rock typing. Remarkably, similar behaviors are expected when *in situ* conditions are taken into account.

3.3 Well placement and layouts

After zoning the reservoir through discrete rock typing, special locations are found within the domain of the high-performance clusters. These points are considered as flow convergence zones susceptible to well placement. In this paper, we have estimated a series of high-performance points which, altogether, form a production layout of single perforations throughout the oilfield. Although the feasibility of implementing wide-scale production strategies in this manner is somewhat improbable because of high project costs, relevant outcomes can be recognized when studying the effects that petrophysical and flow variables cause on optimized well placement. A generic 3D view that shows how the wells are placed in each case is depicted in Fig. 6. In Fig. 7, we have plotted each one of the high-performance well layouts resulting from the averaging rules used in combination with the DRT (left column) and DRT^* (right column) clustering. Color tones stand for different rock types obtained from the same average. Since we are considering only vertical wells, the plots resort to a simplified superior view, by which the location of each point is more easily identified.

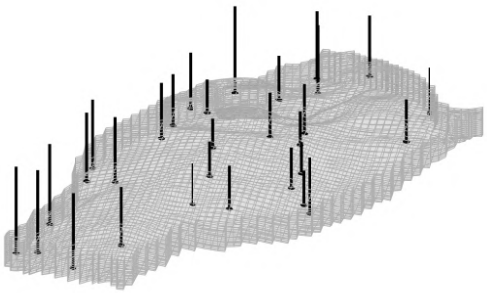

Figure 6. Generic 3D view of the UNISIM-I-D reservoir model with well heads and placement at special locations that cover the whole field.

Note that only the high-performance clusters appear in the figure area even though the rock type range is larger for the considered cases. Numbers are used to label the cluster index. In the second row, for example, green tones concern to clusters generated with computing the geometric average for the permeability. For this average, the best clusters permeated the DRT values 12, 13, 14 and 15, but only the DRT^* values 8, 9 and 10.

Several interesting behaviors take place while comparing the well layouts produced by each clustering/averaging rule, so that we can enumerate a few. The DRT^* approach produces less rock types than DRT, but its cluster distribution is not necessarily restrained. Oppositely, it scatters throughout the oilfield. Moreover, the distributions of the special points computed through the DRT^* clustering have "shadows" of the DRT distributions in the sense of covering common regions of the oilfield. This is weakly observed only in the case of the arithmetic average and under a lower degree in the case of the quadratic average. Production analyses will be performed in the next section.

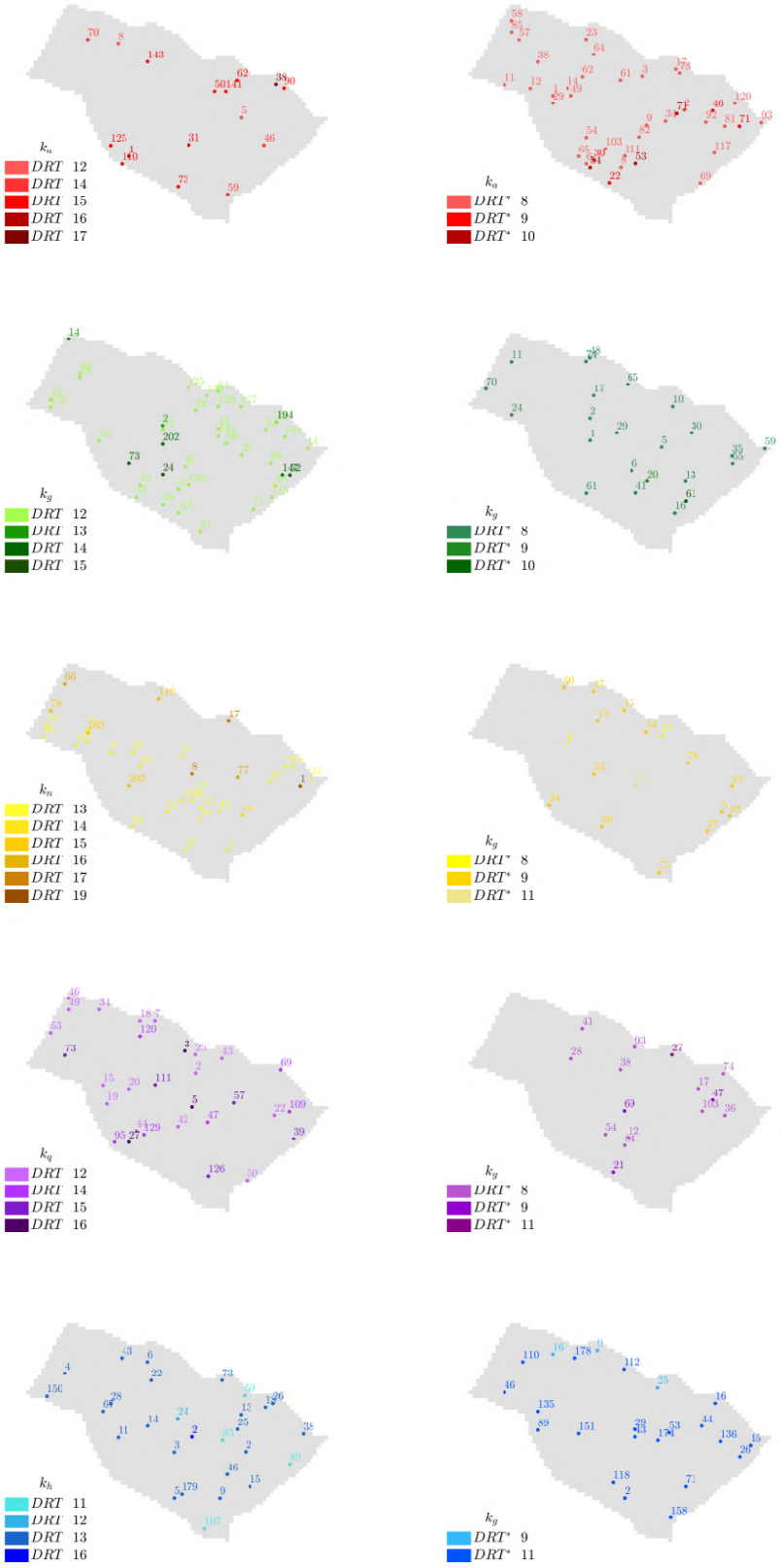

Figure 7. 2D view of sweet spots as a result of the rock clustering guided by each averaging rule/flow indicator pair. The numbers labeling the points correspond to cluster indices.

3.4 Numerical simulations

We have called “sweet spot” each one of the special points determined through the procedures of clustering discussed in the previous sections. The points are associated to a unique computational hydraulic flow unit formed by the union

of cells. Numerically, perforations are opened in those cells whose logical addresses match the sweet spots. In this section, we report flow simulation outcomes obtained through the black-oil module implemented in the MRST (*Matlab Reservoir Simulation Toolbox*) introduced in Krogstad *et al.* (2015) for wells located at the sweet spots, thus forming widespread layouts driven by the clustering/averaging methodology. The curves examined correspond to joint cumulative oil productions in standard barrels and are plotted in Fig. 8. We have set a time range of 20 years for the simulation over ia model initially saturated in oil by about 87%. As seen, the permeability averaging rules have a considerable impact over the produced oil volume not only for layouts obtained with the same flow indicator, but also for layouts compared *vis-à-vis* between the two flow indicators. For the approach DRT, the joint performances can be ordered, in terms of averaging rule, from the largest to the smallest production as k_q, k_g, k_n, k_h, k_a. Oppositely, for the approach DRT^*, the ordering is k_q, k_a, k_n, k_g, k_h. From this, the following comments can be drawn:

- The full layout of the DRT approach was made up by wells quantitatively distributed per averaging rule as 30, 40, 33, 28 and 30 (a total of 161 wells) with ultimate production volume within the range $5 \times 10^8 - 1.4 \times 10^9$ barrels. Likewise, the full layout of the DRT^* approach was formed by wells distributed as 15, 41, 17, 23 and 23 (a total of 119 wells) with ultimate production volume within the range $1 \times 10^8 - 1.4 \times 10^9$. That is to say, the number of wells placed according to the DRT approach is larger, thus boosting up the global production.

- The placement of more wells is not necessarily an indication of superiority. For example, for DRT^*, the averaging rule k_q had the best performance with 15 wells, whereas the rule k_h had the worst performance with 23 wells. Similar conclusion is inferred when comparing k_q and k_g for DRT, for example. The former had the best performance with 30 wells; the latter had a weaker performance with 40 wells.

- With the DRT^* approach, a downward trend is observed in the production curves when compared to DRT. In the first case, except the curve for k_q, all of the others lie below those obtained with the second case. Moreover, k_n, k_g and k_h are shifted down by a considerable difference. This is rather consistent with Eq. (6), since the FZI^* is a reduction of FZI by a factor (the pore-to-matrix ratio).

- Not at all, the curves could be considered as of low performance. All of them demonstrate a profitable production. However, the DRT approach gave more balanced and competitive results.

- Seemingly, the DRT^* approach was more sensitive to changes in the averaging rule, since the production volumes were much more dispersed. However, for k_a and k_q, the productions were as comparable as for the DRT approach.

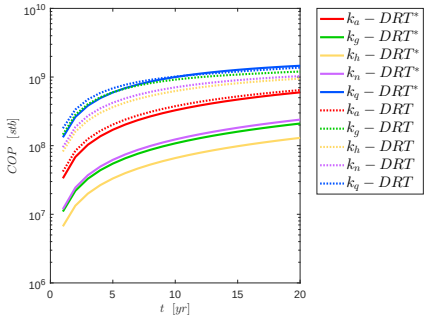

Figure 8. Joint cumulative oil production for all the strategic wells found through the averaging rules and flow indices.

4. CONCLUSION

As discussed in this paper, the variability of the rock types as a function of the permeability averaging rules may be considerably high. The keypoint of this paper relied on contrasting well placement strategies provided by the joint application of a cell-connected rock clustering technique along with a global zoning of flow units through flow indicators. The first approach has considered a classical method known as FZI. The second one has resorted to a newly interpretation of FZI turned to characterization of dynamic flow units. This study has concluded that prolific volumes of produced oil can be attained by using both approaches, but with clear differences when simulated over a long time range. It is not determined yet how far one approach is from another in terms of zoning quality and efficiency. Due to the idealized conditions imposed to the model, such as high oil saturation, light oil viscosity and disregard of thermal and stress effects, many other investigations must be conducted with much more variables. For now, we have verified how sensitive the production predictions can be when different interpretations for flow units are taken into account during reservoir zoning and preparation for flow simulations. Disparities in workflows bring a strong impact over oil and gas industry as it affects the way how exploration, appraisal and development of oilfields are planned. Many challenges exist to reach

sound perfectionism in reservoir modelling. In future studies, we will examine other rock typing methods, near field effects around production columns, multilateral well placement, surrogate models and their integration with artificial intelligence.

5. ACKNOWLEDGEMENTS

G.P.O, L.C.S and W.L.R. thank to CENPES/Petrobras S.A. for funding this research. M.R.B.S acknowledges the financial support of the Brazilian Society of Mechanical Sciences - ABCM.

6. RESPONSIBILITY NOTICE

The authors are the only responsible for the printed material included in this paper.

7. REFERENCES

Amaefule, J. *et al.*, 1993. "Enhanced reservoir description: using core and log data to identify hydraulic (flow) units and predict permeability in uncored intervals/wells". In *SPE-26436-MS: SPE Annual Technical Conference and Exhibition*. Society of Petroleum Engineers.

Baker, R., Yarranton, H. and Jensen, J., 2015. *Practical Reservoir Engineering and Characterization*. Gulf Professional Publishing.

Bangerth, W., Klie, H., Wheeler, M., Stoffa, P. and Sen, M., 2006. "On optimization algorithms for the reservoir oil well placement problem". *Computational Geosciences*, Vol. 10, No. 3, pp. 303–319.

Carman, P., 1937. "Fluid flow through granular beds". *Transactions-Institution of Chemical Engineeres*, Vol. 15, pp. 150–166.

Guo, G. *et al.*, 2005. "Rock typing as an effective tool for permeability and water-saturation modeling: a case study in a clastic reservoir in the oriente basin". In *SPE 97033 - PA: SPE Annual Technical Conference and Exhibition*. Society of Petroleum Engineers.

Hearn, C. *et al.*, 1984. "Geological factors influencing reservoir performance of the hartzog draw field, wyoming". *Journal of Petroleum Technology*, Vol. 36, No. 08, pp. 1–335.

Krogstad, S., Lie, K.A., Møyner, O., Nilsen, H.M., Raynaud, X., Skaflestad, B. *et al.*, 2015. "Mrst-ad–an open-source framework for rapid prototyping and evaluation of reservoir simulation problems". In *SPE reservoir simulation symposium*. Society of Petroleum Engineers.

Mirzaei-Paiaman, A., Ostadhassan, M., Rezaee, R., Saboorian-Jooybari, H. and Chen, Z., 2018. "A new approach in petrophysical rock typing". *Journal of Petroleum Science and Engineering*, Vol. 166, pp. 445–464.

Mirzaei-Paiaman, A., Sabbagh, F., Ostadhassan, M., Shafiei, A., Rezaee, R., Saboorian-Jooybari, H. and Chen, Z., 2019. "A further verification of fzi* and psrti: Newly developed petrophysical rock typing indices". *Journal of Petroleum Science and Engineering*, Vol. 175, pp. 693–705.

Mirzaei-Paiaman, A., Saboorian-Jooybari, H. and Pourafshary, P., 2015. "Improved method to identify hydraulic flow units for reservoir characterization". *Energy Technology*, Vol. 3, No. 7, pp. 726–733.

Nasrabadi, H., Morales, A. and Zhu, D., 2012. "Well placement optimization: A survey with special focus on application for gas/gas-condensate reservoirs". *Journal of Natural Gas Science and Engineering*, Vol. 5, pp. 6–16.

Oliveira, G., Roque, W., Araújo, E., Diniz, A., Simões, T. and Santos, M., 2016. "Competitive placement of oil perforation zones in hydraulic flow units from centrality measures". *Journal of Petroleum Science and Engineering*, Vol. 147, pp. 282–291.

Rahmanifard, H. and Plaksina, T., 2018. "Application of artificial intelligence techniques in the petroleum industry: a review". *Artificial Intelligence Review*, pp. 1–24.

Renard, P. and de Marsily, G., 1997. "Calculating equivalent permeability: a review". *Advances in water resources*, Vol. 20, No. 5-6, pp. 253–278.

Roque, W., Oliveira, G., Santos, M. and Simões, T., 2017. "Production zone placements based on maximum closeness centrality as strategy for oil recovery". *Journal of Petroleum Science and Engineering*, Vol. 156, pp. 430–441.

Soleymanzadeh, A., Parvin, S. and Kord, S., 2019. "Effect of overburden pressure on determination of reservoir rock types using rqi/fzi, fzi* and winland methods in carbonate rocks". *Petroleum Science*, pp. 1–14.

Tiab, D. and Donaldson, E., 2011. *Petrophysics: theory and practice of measuring reservoir rock and fluid transport properties*. Gulf professional publishing.